J|A|C|S
ARTICLES

Published on Web 08/05/2009

Single Molecule Probing of the Local Segmental Relaxation Dynamics in Polymer above the Glass Transition Temperature

Els Braeken,[†] Gert De Cremer,[†] Philippe Marsal,[‡,§] Gérard Pèpe,[‡] Klaus Müllen,[||] and Renaud A. L. Vallée*,[⊥]

Department of Chemistry and Institute of Nanoscale Physics and Chemistry, Katholieke Universiteit Leuven, Celestijnenlaan 200F, B-3001 Heverlee, Belgium, Centre Interdisciplinaire de Nanoscience de Marseille (UPR 3118, CNRS), Campus de Luminy, Case 913, F-13288 Marseille cedex 09, France, Max-Planck-Institut für Polymerforschnung, Ackermannweg 10, D-55128 Mainz, Germany, and Centre de Recherche Paul Pascal (UPR 8641, CNRS), 115 avenue du docteur Albert Schweitzer, F-33600 Pessac, France

Received March 3, 2009; E-mail: vallee@crpp-bordeaux.cnrs.fr

Abstract: We investigate the temporal dynamics of terrylene diimide molecule with four phenoxy rings (TDI) in a poly(styrene) (PS) matrix in the supercooled regime by use of single molecule spectroscopy. By recording both fluorescence lifetime and linear dichroism observables simultaneously, we show that the TDI dye molecule is a versatile probe of the local dynamics in the polymer. The molecule is able to undergo conformational changes, as indicated by lifetime fluctuations and/or reorientation jumps, as indicated by both observables on different time scales. Owing to molecular mechanics and quantum calculations, we could assign the conformational changes to folding/unfolding event(s) of one or more arms with respect to the conjugated core. We tentatively attribute the different spatial extents of the locally probed motions to the α and β relaxation processes occurring in the PS matrix.

Introduction

Understanding the mechanisms responsible for the tremendous slowing down of the mobility when approaching the glass transition is one of the most important challenges in modern soft condensed matter physics, both for low molecular weight and polymeric materials.[1−5] Amorphous atactic polystyrene (PS) is one of the most widely used industrial plastics and a classical example of a mechanically brittle polymer. As such, it is perfectly suited for investigating the connection between the local chemical and physical microstructure and the macroscopic mechanical behavior. Rotational motions of both backbone segments and side groups are the principal relaxation mechanisms in amorphous polymers. Such relaxation processes have been studied experimentally in amorphous PS in the vicinity of the glass-transition temperature T_g by viscosity,[6] compliance,[6] quasielastic neutron scattering,[7] NMR,[8−10] photon correlation spectroscopy,[11,12] dielectric relaxation,[13−15] photobleaching,[16] and second harmonic generation techniques.[17,18] It has been established that above the PS glass-transition temperature (T_g = 373 K), the α-relaxation is the primary relaxation process for the collective motion of polymer segments. At lower temperature, the so-called β process appears.[4] Different opinions about the nature of the β-relaxation exist. Usually this process is attributed to the rotational vibration of backbone segments, but some authors have assigned the β process to the rotations of side phenyl groups. Our aim in this paper is to investigate the differences in local segmental dynamics in a polystyrene melt slightly above the glass transition temperature. In order to perform this task, we use a very versatile method based on the single molecule spectroscopy (SMS) of a dedicated probe.

Because it allows bypassing the ensemble averaging intrinsic to bulk studies, SMS constitutes a powerful tool to assess the dynamics of heterogeneous materials at the nanoscale level.[19−22]

[†] Katholieke Universiteit Leuven.
[‡] Centre Interdisciplinaire de Nanoscience de Marseille.
[§] Present address: Laboratory for Chemistry of Novel Materials, University of Mons-Hainaut, Place du Parc 20, B-7000 Mons, Belgium.
[||] Max-Planck-Institut für Polymerforschnung.
[⊥] Centre de Recherche Paul Pascal.

(1) Jäckle, J. *Rep. Prog. Phys.* **1986**, *49*, 171.
(2) Götze, W.; Sjögren, L. *Rep. Prog. Phys.* **1992**, *55*, 241.
(3) See Debenedetti, P. G. In *Metastable Liquids*; Princeton Univ. Press: Princeton, 1997.
(4) See Donth, E.-W. In *The Glass Transition. Relaxation Dynamics in Liquids and Disordered Materials*; Springer: Berlin, 2001.
(5) See Binder, K.; Kob, W. In *Glassy Materials and Disordered Solids. An Introduction to Their Statistical Mechanics*; World Scientific: Singapore, 2005.
(6) Plazek, D. J. *J. Phys. Chem.* **1965**, *69*, 3480.
(7) Kanaya, T.; Kawaguchi, T.; Kaji, K. *J. Chem. Phys.* **1996**, *104*, 3841.
(8) Pschorn, U.; Rossler, E.; Kaufmann, S.; Sillescu, H.; Spiess, H. W. *Macromolecules* **1991**, *24*, 398.
(9) Kuebler, S. C.; Heuer, A.; Spiess, H. W. *Phys. Rev. E* **1997**, *56*, 741.
(10) He, Y.; Lutz, T. R.; Ediger, M. D.; Ayyagari, C.; Bedrov, D.; Smith, G. D. *Macromolecules* **2004**, *37*, 5032.
(11) Lee, H.; Jamieson, A. M.; Simha, R. *Macromolecules* **1979**, *12*, 329.
(12) Patterson, G. D.; Lindsey, C. P. *J. Chem. Phys.* **1979**, *70*, 643.
(13) Saito, S.; Nakajima, T. *J. Appl. Polym. Sci.* **1959**, *4*, 93.
(14) Fukao, K.; Miyamoto, Y. *J. Non-Cryst. Solids* **1994**, *172−174*, 365.
(15) León, C.; Ngai, K. L.; Roland, C. M. *J. Chem. Phys.* **1999**, *110*, 11585.
(16) Inoue, T.; Cicerone, M. T.; Ediger, M. D. *Macromolecules* **1995**, *28*, 3425.
(17) Dhinojwala, A.; Wong, G. K.; Torkelson, J. M. *J. Chem. Phys.* **1994**, *100*, 6046.
(18) Hall, D. B.; Deppe, D. D.; Hamilton, K. E.; Dhinojwala, A.; Torkelson, J. M. *J. Non-Cryst. Solids* **1998**, *235−237*, 48.
(19) Moerner, W. E.; Orrit, M. *Science* **1999**, *283*, 1670.

By using two-dimensional (2D) orientation techniques, the in-plane (of the sample) projection of the transition dipole moment of the single molecule (SM) [the so-called linear dichroism $d(t)$] has been followed in time and its time correlation function $C_d(t)$ has been computed and fitted by a stretched exponential function $f(t) = \exp[-(t/\tau)^{\beta}]$.[23−26] These investigations have allowed identifying static and dynamic heterogeneity in the samples;[27,28] i.e., SMs exhibit τ and β values varying according to (i) their actual position in the matrix and (ii) the time scale at which they are probed, as a result of the presence of different nanoscale environments. Zondervan et al.[29] investigated the rotational motion of perylene diimide in glycerol. Observations of environmental exchanges were very scarce. They assumed that glycerol consists of heterogeneous liquid pockets separated by a network of solid walls. This was confirmed by conducting rheology measurements at very weak stresses of glycerol and *o*-terphenyl.[30] With 3D orientation techniques, the emission transition dipole moment of a SM has been recorded as a function of time.[31−34] In particular, the distribution of nanoscale barriers to rotational motion has been assessed by means of SM measurements[35] and related to the spatial heterogeneity and nanoscopic α-relaxation dynamics deep within the glassy state. Owing to the high barriers found in the deep glassy state, only few SMs were able to reorient, while somewhat lower barriers could be overcome when increasing the temperature.

Following the temporal evolution of the fluorescence lifetime of single molecules with quantum yield close to unity, we have shown that this observable is highly sensitive to changes in local density occurring in a polymer matrix.[36−41] Using free volume theories, we have related the lifetime fluctuations to hole (free-volume) distributions and determined the number of polymer segments involved in a rearrangement cell around the probe molecule as a function of temperature,[36,39] solvent content,[37] and film thickness.[38] On the basis of a microscopic model for the fluctuations of the local field,[40] we have established a clear correlation between the fluorescence lifetime distributions measured for single molecules and the local fraction of surrounding holes both in the glassy state and in the supercooled regime for various molecular weight oligo(styrene).[41] Furthermore, fluorescence lifetime trajectories of single probe molecules embedded in a glass-forming PS melt exhibit strong fluctuations of a hopping character. Using MD simulations targeted to explain these fluctuations,[42] we have shown that the lifetime fluctuations correlate strongly with the meta-basin transitions in the potential energy landscape of the matrix particles, thus providing a new tool for the experimental study of long-standing issues in the physics of the glass transition. Finally, the interaction between the probe molecule and the polymer matrix can also be investigated. The interaction between carbocyanine dyes and poly(styrene) (PS) polymer chains has been investigated.[43,44] We have shown that the existence of different conformations of such dyes, stabilized owing to favorable interactions with the surrounding polymer matrix, lead to specific spectroscopic responses, i.e., specific fluorescence lifetimes and emission spectra. We found that the type of conformer found in the matrix and its interaction with the surrounding chains governed the local packing of the matrix and thus allows one to probe the local free volume.

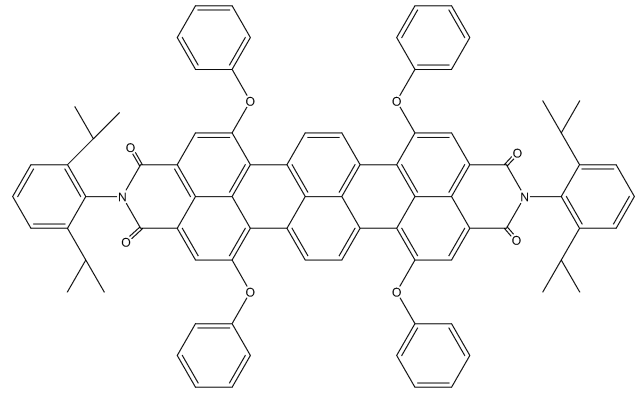

Figure 1. Schematic structure of the terrylene diimide with four phenoxy rings (TDI) dye molecule.

In this paper, we use both 2D orientation techniques and fluorescence lifetime measurements to investigate the mobility of tetraphenoxyterrylene diimide (TDI) molecules (Figure 1) in a low molecular weight ($M_w = 1000$ g mol^{-1}, $T_g \approx 10$ °C) PS matrix. The measurements are performed at room temperature ($T = 19$ °C), thus slightly in the supercooled regime. This allows the dye to reorient substantially during the measurement time. By simultaneously measuring the fluorescence lifetime and linear dichroism trajectories, we can correlate the fluctuations exhibited by both observables. In particular, we can assign jumps occurring simultaneously in both trajectories to reorientational

(20) Xie, X. S.; Trautman, J. K. *Annu. Rev. Phys. Chem.* **1998**, *49*, 441.
(21) Kulzer, F.; Orrit, M. *Annu. Rev. Phys. Chem.* **2004**, *55*, 585.
(22) Vallée, R. A. L.; Cotlet, M.; Hofkens, J.; De Schryver, F. C.; Müllen, K. *Macromolecules* **2003**, *36*, 7752.
(23) Deschenes, L. A.; Vanden Bout, D. A. *J. Phys. Chem. B* **2002**, *106*, 11438.
(24) Tomczak, N.; Vallée, R. A. L.; van Dijk, E. M. H. P.; García-Parajó, M.; Kuipers, L.; van Hulst, N. F.; Vancso, G. J. *Eur. Polym. J.* **2004**, *40*, 1001.
(25) Schob, A.; Cichos, F.; Schuster, J.; von Borczyskowski, C. *Eur. Polym. J.* **2004**, *40*, 1019.
(26) Mei, E.; Tang, J.; Vanderkooi, J. M.; Hochstrasser, R. M. *J. Am. Chem. Soc.* **2003**, *125*, 2730.
(27) Ediger, M. D. *Annu. Rev. Phys. Chem.* **2000**, *51*, 99.
(28) Richert, R. *J. Phys.: Condens. Matter* **2002**, *4*, R703.
(29) Zondervan, R.; Kulzer, F.; Berkhout, G. C. G.; Orrit, M. *Proc. Natl. Acad. Sci. U.S.A.* **2007**, *104*, 12628.
(30) Zondervan, R.; Xia, T.; van der Meer, H.; Storm, C.; Kulzer, F.; van Saarloos, W.; Orrit, M. *Proc. Natl. Acad. Sci. U.S.A.* **2008**, *105*, 4993.
(31) Dickson, R. M.; Norris, D. J.; Moerner, W. E. *Phys. Rev. Lett.* **1998**, *81*, 5322.
(32) Sick, B.; Hecht, B.; Novotny, L. *Phys. Rev. Lett.* **2000**, *85*, 4482.
(33) Lieb, A.; Zavislan, J. M.; Novotny, L. *J. Opt. Soc. Am. B* **2004**, *21*, 1210.
(34) Böhmer, M.; Enderlein, J. *J. Opt. Soc. Am. B* **2000**, *20*, 554.
(35) Bartko, A. P.; Xu, K.; Dickson, R. M. *Phys. Rev. Lett.* **2002**, *89*, 026101.
(36) Vallée, R. A. L.; Tomczak, N.; Kuipers, L.; Vancso, G. J.; van Hulst, N. F. *Phys. Rev. Lett.* **2003**, *91*, 038301.
(37) Vallée, R. A. L.; Tomczak, N.; Kuipers, L.; Vancso, G. J.; van Hulst, N. F. *Chem. Phys. Lett.* **2004**, *384*, 5.
(38) Tomczak, N.; Vallée, R. A. L.; van Dijk, E. M. H. P.; Kuipers, L.; van Hulst, N. F.; Vancso, G. J. *J. Am. Chem. Soc.* **2004**, *126*, 4748.
(39) Vallée, R. A. L.; Tomczak, N.; Vancso, G. J.; Kuipers, L.; van Hulst, N. F. *J. Chem. Phys.* **2005**, *122*, 114704.
(40) Vallée, R. A. L.; Van der Auweraer, M.; De Schryver, F. C.; Beljonne, D.; Orrit, M. *ChemPhysChem* **2005**, *6*, 81.
(41) Vallée, R. A. L.; Baruah, M.; Hofkens, J.; De Schryver, F. C.; Boens, N.; Van der Auweraer, M.; Beljonne, D. *J. Chem. Phys.* **2007**, *126*, 184902.
(42) Vallée, R. A. L.; Van der Auweraer, M.; Paul, W.; Binder, K. *Phys. Rev. Lett.* **2006**, *97*, 217801.
(43) Vallée, R. A. L.; Marsal, P.; Braeken, E.; Habuchi, S.; De Schryver, F. C.; Van der Auweraer, M.; Beljonne, D.; Hofkens, J. *J. Am. Chem. Soc.* **2005**, *127*, 12011.
(44) Braeken, E.; Marsal, P.; Vandendriessche, A.; Smet, M.; Dehaen, W.; Vallée, R. A. L.; Beljonne, D.; Van der Auweraer, M. *Chem. Phys. Lett.* **2009**, *472*, 48.

jumps of the dye molecules. On the contrary, jumps only occurring in the fluorescence lifetime trajectories can be assigned to conformational changes of the TDI molecule, related to the folding of one or more phenoxy arms on the conjugated core. These findings are confirmed by molecular mechanics and quantum chemical calculations dedicated to the determination of the possibly allowed conformations of the dye molecule and their expected spectroscopic properties. The use of such a versatile dye, able to either reorient or change conformation in the PS melt, combined with the simultaneous measurement of fluorescence lifetime and linear dichroism observables, shed light in a unique way on the differences in local segmental dynamics possibly related to the α- and β-relaxation mechanisms.

Experimental Methods

Steady state absorption and emission spectra of TDI in toluene were recorded for concentrations of ca. 10^{-6} M. The absorption measurements were carried out on a Perkin-Elmer Lambda 40 UV/vis spectrophotometer. Corrected emission spectra were recorded on a SPEX fluorolog.

A PS (M_w = 1000 g mol^{-1}, T_g = 10 °C, Polymer Source Inc.) solution of 10 mg/mL in toluene (Sigma Aldrich, spectrophotometric grade) was used to make solutions of nanomolar (10^{-9} M) concentrations of TDI (Figure 1) in PS. Besides this hydrophobic solution, a hydrophilic 10 mg/mL solution of poly(vinyl alcohol) (PVA, M_w = 130 000, Clariant) in water was also prepared. The samples were prepared by spin-coating, at a rate of 1000 rpm, a layer of TDI in PS in between two layers of PVA, situated on the bottom and on top of the PS layer, respectively. This procedure ensured that the TDI dye molecules embedded in the PS layer will not be exposed to either the polymer−glass or the air−glass interfaces, thus avoiding possible electromagnetic boundary effects to interfere on the subsequent measurement of fluorescence lifetimes. Indeed, it has been shown that the fluorescence lifetime of a dye molecule can increase significantly when it is situated close to the polymer−air interface, especially if the transition dipole of the molecule is perpendicular to the interface.[45−47]

The measurements were performed with an inverted confocal fluorescence microscope (Olympus IX 70), with a 100× oil immersion objective (Olympus, NA = 1.3). As an excitation source, a Picoquant pulsed diode laser producing 90 ps pulses of 644 nm, with a repetition rate of 10 MHz was used. This wavelength was well-suited to excite the dye molecule close to its absorption maximum (Figure 2) and the excitation power was set to 1 μW at the entrance of the microscope. The emission signal was separated from the excitation light, circularly polarized by a dichroic filter (DC-Q-600-LP, Chroma) and a long pass filter (HQ600LP, Chroma) in order to get the maximum integrated signal of the emission spectrum (Figure 2), and split into parallel ($I_{||}$) and orthogonal ($I_\perp$) components owing to a 50/50% beam splitter. The emission signal was collected by two avalanche photodiodes (SPCM-AQ-15, EG & G Electro Optics) equipped with a time-correlated single photon counting card (TCSPC card, Becker & Hickl GmbH, SPC 630) used in FIFO mode in order to subsequently determine fluorescence lifetimes. The sample was scanned with a piezo-controlled scanning stage (Physics Instruments), and the instrumental response function of the system is ≈500 ps. The bin times used to build the decay profiles for the molecules were set to 100 ms in order to have at least 500 counts in the decay. This is the minimum number of counts that is needed to fit the decays using the maximum likelihood

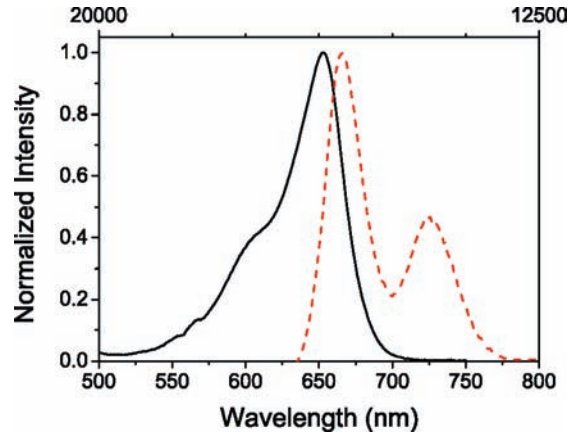

Figure 2. Steady-state absorption and emission spectra of TDI in a toluene solution.

estimation method.[48] The linear dichroism was measured according to the usual formula:

$$d(t) = \frac{I_{||} - GI_\perp}{I_{||} + GI_\perp} \quad (1)$$

in which G is a correction factor accounting for the difference in sensitivity between the two detectors. The correction factor is determined by using a homogeneous fluorescent sample (a sample with high concentration of dye molecules) and dividing $I_{||}$ by $I_\perp$.

The measurements were performed at room temperature, which is above the glass transition temperature of the PS used.

Theoretical Methods

Geometries and conformations of TDI are issued from GenMol calculations. GenMol is a software based upon molecular mechanics[49] except for the atomic charge calculations that are issued from semiempirical approximations.[51,52] A genetic algorithm is used to find the preferred conformations of the molecule. A molecule conformation is described by N torsion angles, with values α_i. A preferred conformation (corresponding to a minimum of the strain energy) of a molecule is thus characterized by a unique set of α_i values. For bonds not belonging to rings, complete rotations are allowed around σ bonds. Only partial rotations around σ bonds with a π character conformation are permitted, in order to stay close to the planarity. Each torsion angle value is considered as one gene. The algorithm used to find the preferred conformations of a molecule is described elsewhere.[52]

The characterization of the lowest electronic singlet excited states has been performed by the semiempirical Hartree−Fock intermediate neglect of differential overlap (INDO) method as parametrized by Zerner et al.[53] This approximation was used in combination with a single configuration interaction (SCI) methodology. For all calculations, the CI active space has been

(45) Vallée, R.; Tomczak, N.; Gersen, H.; van Dijk, E. M. H. P.; García-Parajó, M. F.; Vancso, G. J.; van Hulst, N. F. *Chem. Phys. Lett.* **2001**, *348*, 161.
(46) Schroeyers, W.; Vallée, R.; Patra, D.; Hofkens, J.; Habuchi, S.; Vosch, T.; Cotlet, M.; Müllen, K.; Enderlein, J.; De Schryver, F. C. *J. Am. Chem. Soc.* **2004**, *126*, 14310.
(47) Enderlein, J. *Chem. Phys.* **1999**, *247*, 1.
(48) Maus, M.; Hofkens, J.; Gensch, T.; De Schryver, F. C.; Schaffer, J.; Seidel, C. *Anal. Chem.* **2001**, *73*, 2078.
(49) See Pèpe, G.; Siri, D. In *Modeling of Molecular Structures and Properties Studies in Physical and Theoretical Chemistry*; Rivail, J. L., Eds.; Elsevier B. V.: Amsterdam, 1990.
(50) Pèpe, G.; Perbost, R.; Courcanbeck, J.; Jouanna, P. *J. Cryst. Growth* **2009**, *311*, 3498.
(51) Del Re, G. *J. Chem. Soc.* **1958**, *40*, 4031.
(52) Pèpe, G.; Serres, B.; Laporte, D.; Del Re, G.; Minichino, C. *J. Theor. Biol.* **1985**, *115*, 571.
(53) Zerner, M. C.; Loew, G.; Kichner, R.; Mueller-Westerhoff, U. T. *J. Am. Chem. Soc.* **2000**, *122*, 3015.

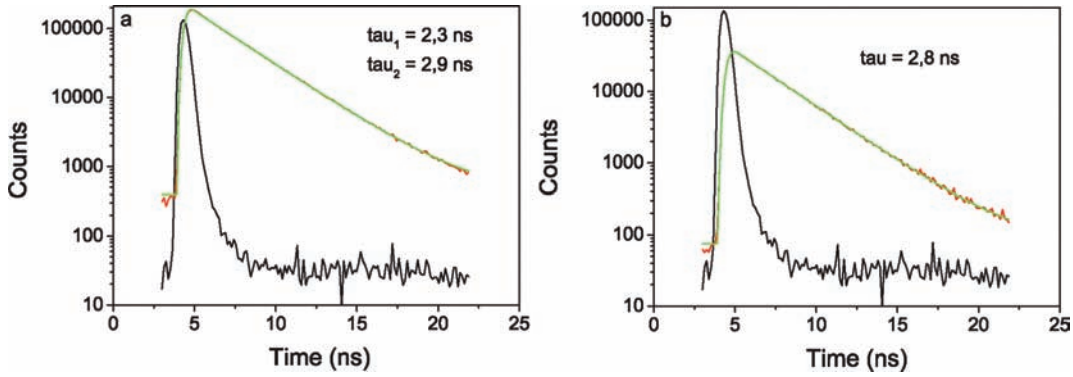

Figure 3. Decay profiles obtained by integrating all photons recorded during the measurement time of a molecule. The profile shown in a was best fit with a biexponential decay model with decay times of $\tau_1 = 2.3$ ns with a contribution of 20% and $\tau_2 = 2.9$ ns with a contribution of 80%. The decay profile shown in b was best fit with a monoexponential decay model with decay time $\tau = 2.8$ ns. The black curve is the instrumental response function of the setup, which has a fwhm of about 0.5 ns.

built by promoting one electron from one of the highest 60 occupied to one of the lowest 60 unoccupied levels.

Results and Discussion

The normalized (relative to the maximum value) absorption and emission spectra of TDI (Figure 1) are shown in Figure 2. The absorption and emission spectra have a maximum around 653 and 666 nm, corresponding to the $S_0 \rightarrow S_1$ and $S_1 \rightarrow S_0$ electronic transitions, respectively.

Single molecule measurements were performed on thin films, spin-coated from a 10^{-9} M solution of TDI in PS/toluene in between two layers of PVA/H_2O. To localize the individual molecules, an area of 10 μm by 10 μm was scanned. Taking into account the number of molecules found in this area and comparing with the expected number to be found for such a low dye concentration (10^{-9} M), we made sure to have the right concentration to measure individual molecules. Furthermore, the diffraction limited spots observed on the scanning areas and the one-step bleaching (not shown) confirm the observation of single molecules. Once localized, fluorescence lifetime and linear dichroism trajectories were recorded for each individual molecule.

In a first step, the decay time(s) of each individual molecule is (are) obtained by integrating all photons recorded during the measurement time of the molecule (until photobleaching irreversibly occurs) in a decay profile. Figure 3 exhibits such profiles for two different molecules. One of the two decay profiles shown was best fit by a biexponential decay model (a) with decay times of 2.3 and 2.9 ns while the other could be best fit by a monoexponential decay model (b) with decay time of 2.8 ns. In all cases, the best fits have been determined on the basis of a careful examination of the χ^2 parameter, visual inspection of the residuals, and autocorrelation of the latter. Figure 4 collects the distribution of decay times obtained by fitting the decay profiles of all measured molecules. Clearly, this distribution is bimodal with peaks centered at $\tau = 2.0$ and 2.9 ns with a respective contribution of 23% and 77%. The recurrent occurrence of these two specific decay times in the decay profiles gives us a strong indication of the probable emission detection of various conformers of the TDI dye molecule.

In a simplistic picture, one may imagine TDI as a conjugated core surrounded by fours arms (phenoxy rings). According to the position of the arms with respect to the conjugated core, one can see five different conformations emerging: the one

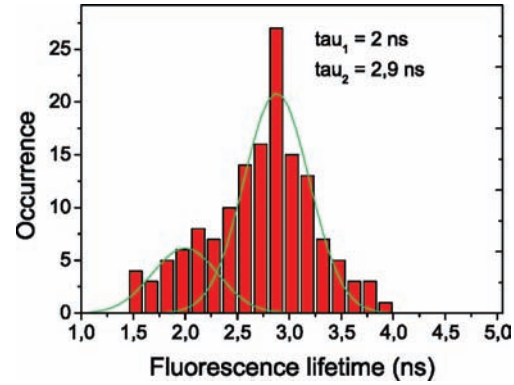

Figure 4. Distribution of the decay times obtained by fitting the decay profiles of all individual molecules either by biexponential or monoexponential decay models, as appropriate.

where all arms are collapsed on the core (hereafter called 0E for zero extended arm) and the ones where one, two, three or the four arms are brought away from the core and thus extended (hereafter called 1E, 2E, 3E, and 4E, depending on the number of arms extending away from the core). Following this simplistic view, changes in transition dipole moment and in transition energy are expected for the different conformations, due to the various extension of the arms, giving rise to various decay times of the dye molecule.

In order to give a theoretical support to this statement, we performed an in-depth theoretical investigation of this molecular system. As pointed out elsewhere,[54] perylene diimide (PDI) molecules substituted in the bay area by four phenoxy groups exhibit several radiative lifetimes depending of the number of phenoxy subtituents strongly interacting with the conjugated core, in an autosolvation scheme. We have demonstrated that this strong interaction led to a coupling of the transition densities, essentially between the two nitrogen atoms of the PDI conjugated core. Depending on the number of folded arms (from zero to four), this coupling of the transition densities can be more or less delocalized on the phenoxy arms, thus strongly modifying the transition dipole of the studied conformer and, in turn, its radiative lifetime.[54] The molecule investigated here is characterized by a longer conjugated core. Performing GenMol[49] molecular mechanic studies of the conformational space, we

(54) Fron, E.; Schweitzer, G.; Osswald, P.; Würthner, F.; Marsal, P.; Beljonne, D.; Müllen, K.; De Schryver, F. C.; Van der Auweraer, M. *Photochem. Photobiol. Sci.* **2008**, *7*, 1509.

Table 1. Calculated Radiative Lifetime and Total Energy of the Different Conformers

n	$S_0 \rightarrow S_1$ transition energy (eV)	total transition dipole	transition dipole *X* (D)	transition dipole *Y* (D)	transition dipole *Z* (D)	radiative lifetime (ns)	energy (kJ/mol)
0	1.941	14.6531	14.6528	0.0564	0.0653	3.9	145.2
1	1.999	14.8115	14.8115	0.2217	−0.172	3.5	153.2
2	1.995	14.8939	14.8852	0.4873	−0.1488	3.5	151.9
3	1.995	14.969	14.9657	0.3058	−0.0767	3.4	151.2
4	1.988	15.1075	15.1073	−0.0085	−0.0602	3.4	150.2

determined the preferred conformations of the molecule. We then used these optimized geometries as starting points for single point INDO/SCI excited states calculations and compute, in this way, the radiative lifetime of each conformer. This approach has already been validated in various studies,[43,44,54] which allowed us to stress, with a high accuracy, the consequences of a change of molecule conformation on the measured radiative lifetime obtained at the single molecule spectroscopy level. In Table 1, we report the computed vertical transition energies, transition dipole moments, energies, and radiative lifetimes of the five selected conformers (Figure 5), depending on the numbers of folded phenoxy units in strong van der Waals interactions with the conjugated core. We can highlight two different groups of conformers. The first group is the molecule with zero extended phenoxy substituents (0E), the most stable conformer, having a long lifetime $\tau = 3.9$ ns and a small energy gap due to a strong energetic stabilization of the π systems owing to favorable interactions with the arms. Such a conformation leads to the smallest computed transition dipole moment, as due to the opposite contributions of the transition dipole moment of the conjugated core and of those of all the phenoxy susbtituents to the total transition dipole moment. The second group is the molecules with nonzero extended (1E, 2E, 3E, or 4E) phenoxy substituents, having a short lifetime $\tau \approx 3.4-3.5$ ns, high energy gap, and a large transition dipole moment due to phenoxy decoupling. Let us strongly stress here that the unfolding of a single arm is enough to provide the full decrease of the computed radiative lifetime, going from 3.9 to 3.4−3.5 ns. In this respect, let us note that several 2E conformers may occur, with the other two phenoxy groups being either below or above the ring system in diagonal or neighboring positions. All these 2E conformers have similar spectroscopic properties. These results are very interesting when contrasted with those obtained for the previously investigated PDI molecule,[54] where the unfolding led to a linear modification of the radiative lifetime with the number of arms extending far away from the conjugated core: in this longer conjugated core, the phenoxy substituents are less polarized by the strongly delocalized transition densities on the conjugated core. This lack of polarization leads to a stronger decoupling of the arms with respect to the conjugated core and, consequently, to a smaller contribution of the arms to the total transition dipole moment and transition energy. Both contributions, in turn, have an opposite effect and lead to similar radiative lifetimes, as soon as the fully symmetric autosolvated conformation (0E) is destroyed.

These calculations have been performed in vacuum. The radiative lifetime in vacuum has been calculated with the usual formula

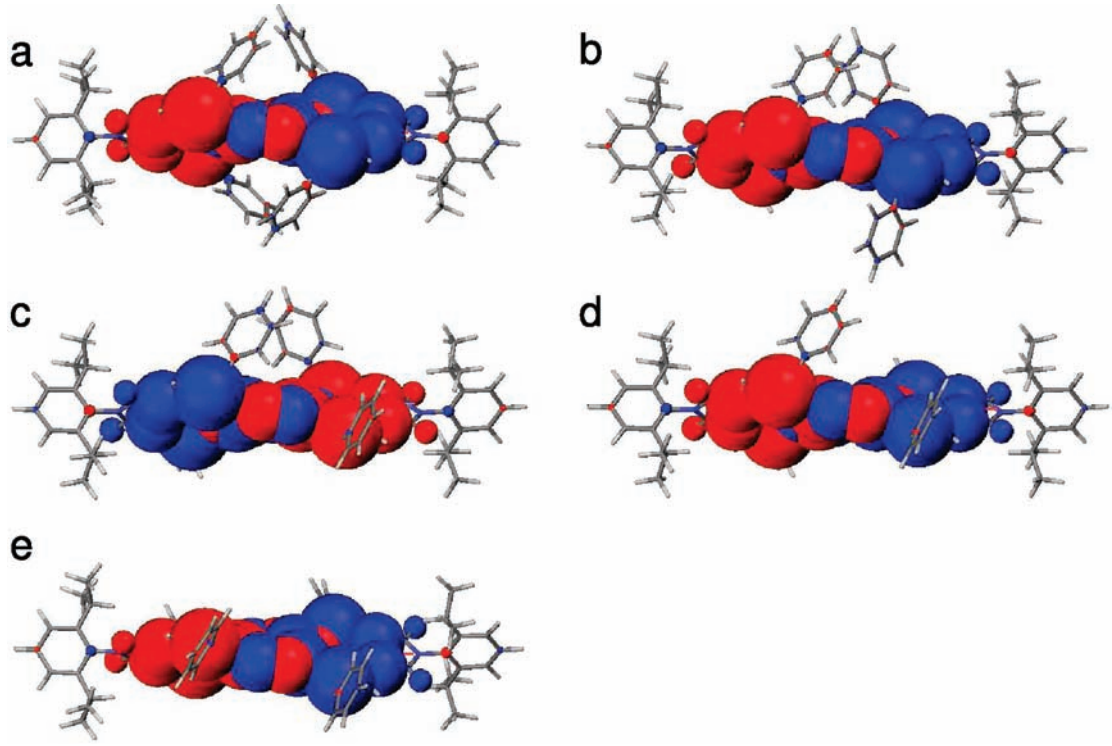

Figure 5. Molecular structures and atomic transition densities associated with the lowest optically allowed electronic excitation for the five most stable conformers of TDI. From a to e, the conformers range from the folded structures (a, 0E) progressively to the completely extended structure (e, 4E). The size of the spheres is proportional to the amplitude of the atomic transition densities.

$$\tau_0 = \frac{m_e \varepsilon_0 {c_0}^3}{2e^2 \pi \nu_0 f} \quad (2)$$

where e is the charge of the electron, ε_0 and c_0 are the permittivity and the speed of light in a vacuum, and ν_0 and f are the transition frequency and the oscillator strength of the probe molecule in a vacuum, respectively.

By further taking into account the renormalization of the photon in the medium, $\varepsilon_0 \rightarrow \varepsilon_r \varepsilon_0$ and $c_0 \rightarrow c_0/n$, the lifetimes are $\tau = 2.5$ ns for the 0E conformation and $\tau = 2.2$ ns for the others, close enough to the experimentally obtained values.

In a second step, the fluorescence lifetime and linear dichroism trajectories have been built for each single molecule, with a binning time of 100 ms. Thus, we did collect the photons in time intervals of 100 ms, calculate both observables for this time interval, and build the time trace as well as the time distribution of both observables for each individual molecule. Furthermore, for each molecule exhibiting significant fluctuations of one or both observables during its measurement time, we did calculate the corresponding autocorrelation function: $C_d(t')$ for the autocorrelation function of the linear dichroism $d(t)$

$$C_d(t') = \frac{\sum_{t=0}^{t=T-t'} d(t+t')\, d(t) - d(\bar{t})\, d(\bar{t})}{\sum_{t=0}^{t=T} d(t)\, d(t) - d(\bar{t})\, d(\bar{t})} \quad (3)$$

where $d(\bar{t})$ is the average value of the linear dichroism on the length T of its time trace. Correspondingly, $C_f(t')$ has been calculated for the autocorrelation function of the fluorescence lifetime $\tau(t)$.

The relaxation times were obtained by either fitting the autocorrelation curves with a monoexponential decay model or by simply reporting the value for which the curve has decayed to one-third of its initial value. The relaxation times obtained indicate the time scale of the fluctuations of the corresponding observable for each individual molecule.

Among the 86 molecules investigated in this study, 11 exhibit nonfluctuating fluorescence lifetime and linear dichroism time traces. Figure 6 shows such a molecule with an average lifetime $\tau = 3$ ns and linear dichroism $d = -0.25$. The distributions of both observables are monomodal and very narrow, indicating a molecule frozen in the matrix during its measurement time (i.e., until irreversible photodissociation of the molecular structure occurs). So, while in the supercooled regime, some 10 °C above its glass transition temperature, the PS matrix can trap TDI molecules for such a long time scale. A molecule of this class exhibited the integrated decay profile shown in Figure 3b.

Contrasting with the previous behavior, Figure 7 shows an example of a molecule with fluctuating lifetime time trace while the linear dichroism time trace remains at a constant value. The lifetime time trace and bimodal distribution clearly indicate transitions between lifetime values peaked at $\tau_1 = 2$ ns and $\tau_2 = 2.8$ ns. On the contrary, the linear dichroism does not change substantially during the experiment (roughly the same time scale as the measurement time for the molecule observed in Figure 6), as best indicated by its monomodal and narrow distribution. The relaxation time obtained from the autocorrelation curve performed for the lifetime observable (Figure 7b) is $\zeta = 2$ s. Nine molecules only showed jumps in the fluorescence lifetime and not in linear dichroism. We attribute this behavior to molecules that are able to perform a conformational change in the matrix, while not able to reorient significantly, and tentatively assign the occurrence of a folding/unfolding event of one or more arms of the TDI dye molecule to uncorrelated motions of lateral phenyl groups of the surrounding PS chains. Such motions, due to the β relaxation mechanism, are expected to occur on shorter time scales than the α relaxation process, involving a collective rearrangement of the PS chain skeletal, only able to bring on a reorientation of the whole TDI probe molecule. An example of integrated decay profile of a molecule belonging to this class is shown in Figure 3a.

In order to test our attempt of attribution, we use the results of the INDO/SCI quantum calculations performed on the optimized calculated geometries to investigate the expected change in linear dichroism related to a change of conformation from the zero extended structure (0E) to one of the unfolded structures (1E, 2E, 3E, or 4E). The X, Y, and Z components for the different conformations are reported in Table 1. Only small changes of the transition dipole moment components are found upon a conformational change. By setting the transition dipole moment vector of the 0E conformer at the origin of a traditional spherical coordinate system,[55] we did measure the changes in linear dichroism occurring due to a change of conformation from the 0E structure to any of the unfolded ones for all colatitude θ angles ranging from 0° to 90° and azimuthal ϕ angles ranging from 0° to 180°, by steps of 15°, in order to also account for the different orientations of the molecule transition dipole moment possibly encountered in the measurements. Figure 8 shows the values of linear dichroism and fluorescence lifetime for a given orientation $\theta = 90°$ and $\phi = 52°$ of the five different conformers. Figure 8 clearly shows that a change of conformation of the TDI molecule may indeed give rise to a bimodal distribution of lifetimes and monomodal distribution of linear dichroism, in accordance with the observations reported in Figure 7.

In a third class, we find 58 molecules for which lifetime fluctuations occur partly simultaneously (correlated) to jumps in linear dichroism and partly independently to any linear dichroism change. Figure 9 exhibits the fluorescence lifetime and linear dichroism trajectories for such a molecule. Some jumps occurring simultaneously in lifetime and linear dichroism are indicated by the vertical dashed lines. The main values of lifetime and dichroism between which the transitions occur are signaled by horizontal lines. We find essentially a bimodal distribution of lifetimes with peaks centered at $\tau = 2.2$ and 2.8 ns and a trimodal distribution of linear dichroism with $d = -0.2$, 0.25, and 0.75. Figure 9a shows that many more fluctuations occur in the lifetime time trace than in the linear dichroism time trace, i.e., in between each simultaneous jump of lifetime and linear dichroism, we can still observe many fluctuations of the lifetime only. This observation is better quantified by analysis of the autocorrelation functions of both observables. While the linear dichroism autocorrelation curve exhibits essentially a one-step decay on a time scale $\zeta = 23$ s, the fluorescence lifetime autocorrelation function presents a two-steps relaxation process, with a first decay to a plateau at $C_f(t) = 0.55$ (see horizontal dotted line in Figure 9b), corresponding to a relaxation time $\zeta \approx 2$ s (see vertical arrow in Figure 9b) followed by a second and final decay with a relaxation time $\zeta = 11$ s. These

(55) Wei, C. J.; Kim, Y. H.; Darst, R. K.; Rossky, P. J.; Vanden Bout, D. A. *Phys. Rev. Lett.* **2005**, *95*, 173001.

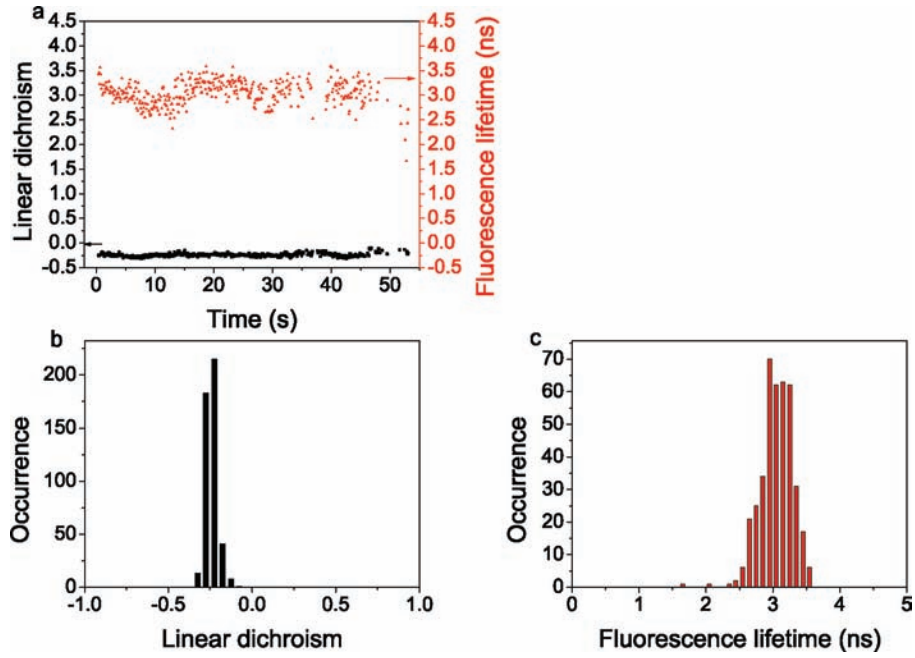

Figure 6. (a) Linear dichroism (black) and fluorescence lifetime (red) trajectories of a molecule that neither reorients nor undergoes conformational changes. (b) Narrow distribution of the linear dichroism trajectory shown in part a with a single peak at $d = -0.25$ (c) Narrow fluorescence lifetime distribution of the trajectory shown in part a with a single peak at $\tau = 3$ ns.

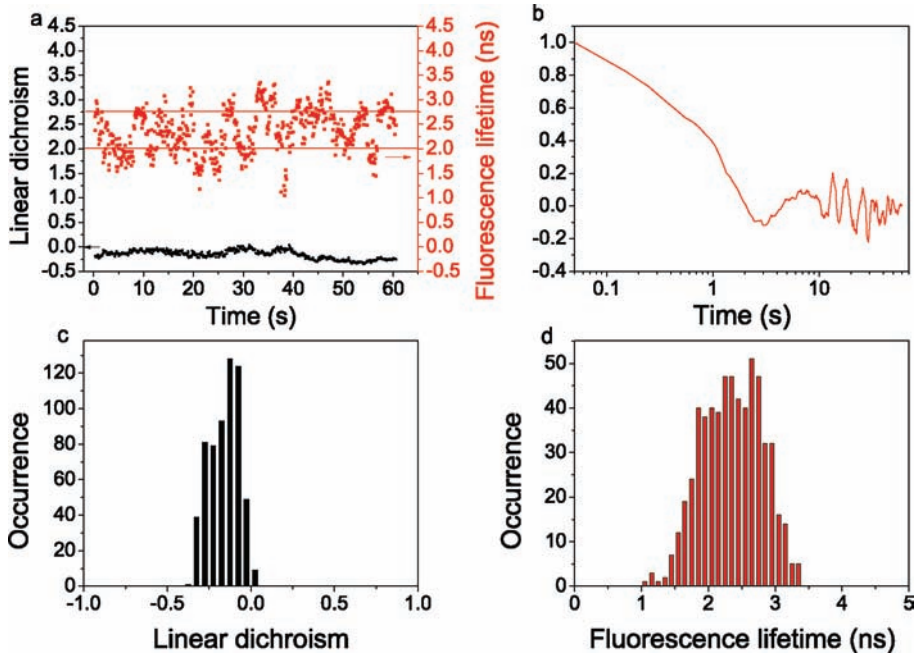

Figure 7. (a) Linear dichroism (black) and fluorescence lifetime (red) trajectories of a molecule that undergoes conformational changes but does not perform a rotational move. The horizontal lines are guidelines for the different levels in fluorescence lifetime. (b) Corresponding correlation curve of the fluorescence lifetime with a relaxation time of 2 s. (c) Distribution of the linear dichroism trajectory shown in part a, which is very narrow and peaks at $d = -0.2$. (d) Fluorescence lifetime bimodal distribution of the trajectory shown in part a with peaks corresponding to the red horizontal lines at values of $\tau = 2$ and 2.75 ns.

observations may be rationalized as follows: the relaxation time corresponding to roughly 2 s and corresponding to the numerous fluctuations of the fluorescence lifetime alone must be attributed to "pure" conformational changes of the TDI probe molecule in a mechanism assisted by the uncorrelated motions of lateral phenyl groups of PS chains, i.e., due to the β-relaxation process in the PS matrix. On this time scale, the molecule does not rotationally move as a whole; hence, the linear dichroism is not modified. Besides these uncorrelated motions and on a longer time scale, roughly 1 order of magnitude slower, the α-relaxation process occurs, where collective segmental rearrangements of the PS backbone give rise to a reorientation of the probe molecule as a whole, mainly accompanied by a conformational change of the probe molecule and signaled by simultaneous jumps of the lifetime and linear dichroism. The slight variations theoretically found in the transition dipole orientation for the different molecular states are so small compared to the reorientation of the molecule as a whole that

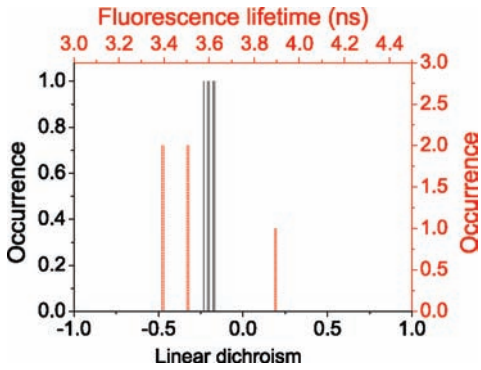

Figure 8. Calculated values of fluorescence lifetime (red) and linear dichroism (black) for the different conformers of TDI for an initial orientation of the 0E conformer at $\theta = 90°$ and $\phi = 52°$.

they are not noticeable experimentally. On average, for the 58 molecules belonging to this class, the correlation times for linear dichroism and fluorescence lifetime corresponding to the long relaxation time attributed to the α-relaxation process are 27 and 8 s, respectively, indicating that the fluorescence lifetime and linear dichroism observables do not probe the α-relaxation mechanism on the same spatial scale. As reported already elsewhere,[16,56−58] the time scale for reorientation indeed greatly depends on the size of the probe and on the particular observable chosen to determine the reorientation dynamics. As such, the linear dichroism relaxation time of a single molecule, as measured on a confocal microscope with a high NA objective, has been shown to correspond to the relaxation time of a second rank [based on $P_2(t)$] reorientational correlation function while the fluorescence lifetime is essentially sensitive to the very first shells of the polymer chains surrounding the probe molecule and thus has a relaxation time corresponding to that of a higher rank [based on $P_l(t)$, $l \geq 4$] reorientational correlation function.[58]

Finally, the fourth class comprises the rare molecules (eight) that exhibit fluorescence lifetime fluctuations only simultaneously to linear dichroism jumps as a result of both reorientations and conformational changes of the dye molecule; i.e., these molecules probe the α-relaxation mechanism without probing the β-relaxation process. Figure 10 shows the lifetime and linear dichroism time traces of such a molecule. Clearly, the jumps observed in both observables always correlate in time. Their distributions are broad and multimodal with peaks centered at $d = -0.2$, 0.1, and 0.35 for the linear dichroism and $\tau = 2.6$ and 3.4 ns for the fluorescence lifetime. The correlation curves of both observables for this molecule are similar with a one-step decay and provide relaxation times $\zeta = 38$ and 57 s for the linear dichroism and fluorescence lifetime, respectively. The average correlation times of linear dichroism and fluorescence lifetime for the eight molecules classified here are 14 and 18 s, respectively.

Figure 11 collects the relaxations times attributed to the α-relaxation process for all molecules reorientating as a whole in the PS matrix and for both observables. Both methods of determination of these relaxation times (fitting the autocorrelation curves with a monoexponential decay model or simply reporting the value for which the curve has decayed to one-third of its initial value) have been used and are shown to match very well: the distributions obtained in both cases are very similar. The correlation times obtained for the fluorescence lifetime are on average shorter than those obtained for the linear dichroism.

At this point, it is interesting to compare our results to those, essentially originating from ensemble measurements, previously reported in the literature. In the past, dynamics associated with the α-relaxation in PS have been probed at and above T_g by a variety of techniques such as viscosity,[6] compliance,[6] quasielastic neutron scattering,[7] NMR,[8–10] photon correlation spectroscopy,[11,12] dielectric relaxation,[13–15] photobleaching,[16] second harmonic generation techniques,[17,18] and molecular dynamic simulations.[10] The relaxation times obtained by these techniques are very similar and are about 1−5 min at T_g while 1 or 2 orders of magnitude faster a few degrees slightly above T_g. The relaxation times obtained here, $\zeta \geq 10-20$ s, are slightly longer than the expected α-relaxation time scale at the working temperature $T_g/T = 0.97$. This slight discrepancy can be explained by the relative size of our probe as compared to the surrounding monomers. Indeed, the TDI molecule investigated in this study is rather huge as compared to the styrene surrounding monomers, and it is a well-known fact[56] that, as the probe molecule exceeds the surrounding constituents in size, the rotational correlation slows down and leads to a significant increase of the rotational time scale.

Concerning the presence of a secondary relaxation process, the so-called β-relaxation process, experimental[11,15] and theoretical[59] studies agree to associate a β-relaxation time scale roughly 3 orders of magnitude faster than the α-relaxation time scale at around T_g. Some previous work by Leon et al.[15] concerning dielectric relaxation measurements of propylene glycol and oligomers having different number (N) of repeat units clearly shows that the separation between the α- and β-relaxations decreases with decreasing N, so it is difficult to resolve the β-relaxation from the more intense α-relaxation in propylene glycol. In this study, we deal with oligomers of a few styrene monomers. The same effect as discussed by Leon et al.[15] could thus explain the "small" 5−10 times ratio between the α- and β-relaxation time scales observed in our case.

One could also ask if we really probe two time scales, given the fact that our trajectories are only 10−50 times longer that the longest decay times actually determined. It is a well-known fact that finite trajectory lengths have a significant influence on the determination of the associated relaxation times.[60] Trajectories only 20 times longer than the determined decay constant lead to errors on this decay constant of about 50%. However, in the case of our study, fluorescence lifetime autocorrelation curves, like the one shown in Figure 9b, clearly exhibit a two-steps behavior with a first decay to a plateau, shown by the dotted line and the arrow in the figure on a time scale of about 2 s, followed by a second decay with a time scale of about 11 s. It is worthwhile to mention here that this behavior has been exhibited for all 58 molecules pertaining to this class. This behavior is also very reminiscent of a theoretical study performed by Lyulin et al.,[59] where the finding of two peaks in the distribution function of relaxation times for the P_2 autocor-

(56) Wang, L.-M.; Richert, R. *J. Chem. Phys.* **2004**, *120*, 11082.
(57) Huang, W.; Richert, R. *Philos. Mag.* **2007**, *87*, 371.
(58) Vallée, R. A. L.; Paul, W.; Binder, K. *J. Chem. Phys.* **2007**, *127*, 154903.
(59) Lyulin, A. V.; Balabaev, N. K.; Michels, M. A. *Macromolecules* **2002**, *35*, 9595.
(60) Lu, C.-Y.; Vanden Bout, D. A. *J. Chem. Phys.* **2006**, *125*, 124701.

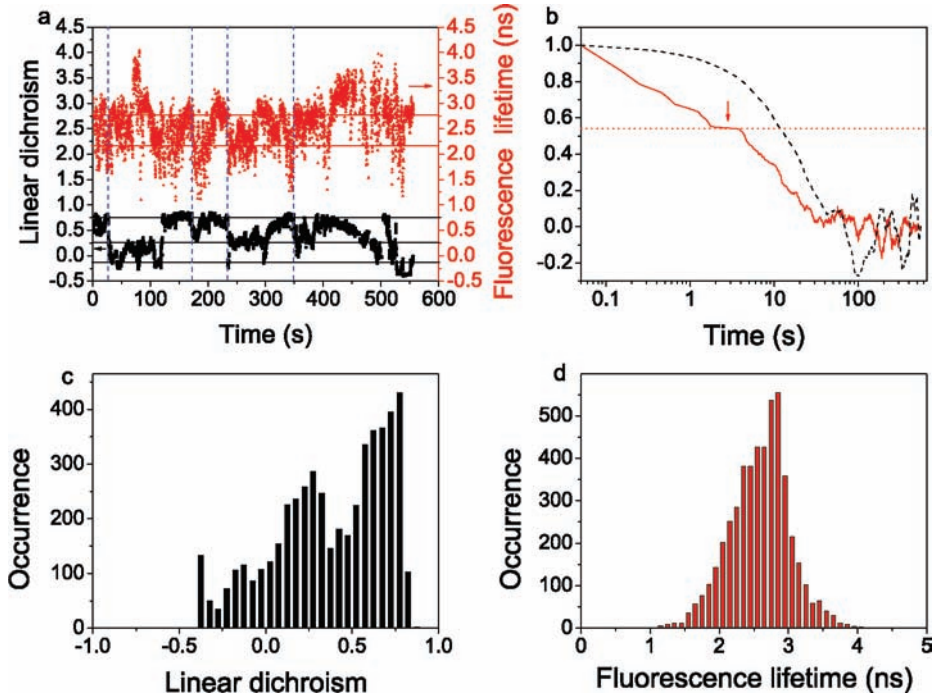

Figure 9. (a) Linear dichroism (black) and fluorescence lifetime (red) trajectories of a molecule that reorients and undergoes conformational changes. The horizontal lines are guidelines for the different levels in linear dichroism (black) and fluorescence lifetime (red). The vertical lines indicate a few correlated jumps occurring simultaneously in linear dichroism and fluorescence lifetime (blue dashed vertical line). (b) Corresponding correlation curves of linear dichroism (black dashed) and fluorescence lifetime (red solid) with relaxation times of 23 and 11 s, respectively. (c) Distribution of the linear dichroism trajectory shown in part a with peaks corresponding to the black horizontal lines at values of $d = -0.2$, 0.25, and 0.75. (d) Fluorescence lifetime distribution of the trajectory shown in part a with peaks corresponding to the red horizontal lines at values of $\tau = 2.2$ and 2.75 ns.

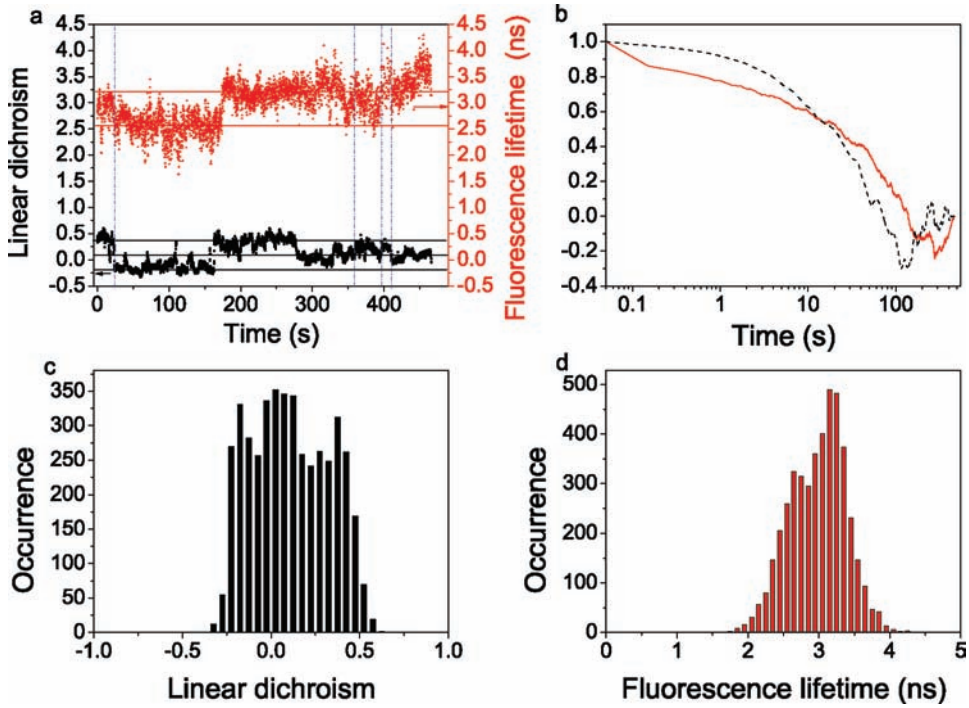

Figure 10. (a) Linear dichroism (black) and fluorescence lifetime (red) trajectories of a molecule that reorients but does not undergo any conformational change not associated with a reorientation of the dye molecule. The horizontal lines are guidelines for the different levels in linear dichroism (black) and fluorescence lifetime (red). The vertical lines indicate a few correlated jumps occurring simultaneously in linear dichroism and fluorescence lifetime (blue dashed vertical line). (b) Corresponding correlation curve of linear dichroism (black dashed) and fluorescence lifetime (red solid) with relaxation times of 38 and 57 s, respectively. (c) Distribution of the linear dichroism trajectory shown in part a with peaks corresponding to the black vertical lines at values of $d = -0.2$, 0.1, and 0.35. (d) Fluorescence lifetime distribution of the trajectory shown in part a with peaks corresponding to the red horizontal lines at values of $\tau = 2.6$ and 3.4 ns.

relation functions in low molecular weight PS slightly above the glass transition has been assigned to the α-relaxation dynamics and to a β-activated process for the slow and fast relaxation times, respectively. Of course, a very interesting

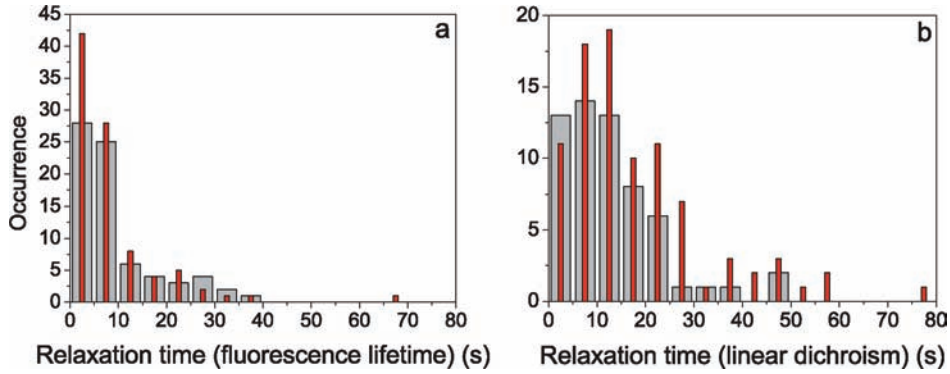

Figure 11. Distribution of correlation times for (a) fluorescence lifetime and (b) linear dichroism. The narrow red bars give the correlation time obtained from taking the relaxation time as the time at which the correlation function has decayed to one-third of its initial value, and the broader gray bars give the correlation times obtained by fitting the autocorrelation curves with an exponential decay model.

perspective of the work performed in this paper would be to perform a temperature-dependent investigation, allowing one to probe the expected non-Arrhenius, Arrhenius types of behavior for the α and β types of relaxation dynamics.

Conclusions

In conclusion, we have shown in this paper that both fluorescence lifetime and linear dichroism of single molecules are observables able to probe the α-relaxation dynamics of the surrounding polymer matrix. The α-relaxation times associated with both observables agree well together and with data reported in the literature concerning ensemble measurements. Furthermore and contrarily to the linear dichroism, the fluorescence lifetime observable of the versatile TDI dye is able to trace small changes occurring in the surrounding polymer matrix, owing to the ability of the TDI phenoxy rings to fold/unfold onto the conjugated core, giving rise to a new conformer, i.e., to a small change of the transition dipole moment orientation, but substantial enough in magnitude to be noticeable by the fluorescence lifetime observable. As such, the β-relaxation process, associated with uncorrelated motions of lateral phenyl groups of PS chains and assigned to be responsible of the folding/unfolding event of one or more arms of the TDI dye molecule, can be probed as well at the single molecule level. It has an average relaxation time of about 2 s, i.e., is 1 order of magnitude slower than the relaxation time associated with the α-relaxation mechanism, under the conditions of this study. Performing single molecule fluorescence spectroscopy experiments with simultaneous determination of the fluorescence lifetime and linear dichroism observables for a dye molecule so versatile as TDI, able to reorient and change conformation, proves thus here to be a unique tool to probe subtle differences in local segmental dynamics related to the α- and β-relaxation mechanisms.

Acknowledgment. The authors are thankful to the FWO for financial support and a postdoctoral fellowship to R.V., to the research council of K. U. Leuven for funding in the framework of GOA 2006/2, and to Belgian Science policy for funding through IAP V/03 and VI/27/. The "Instituut voor de aanmoediging van innovatie door Wetenschap en Technologie in Vlaanderen" (IWT) is acknowledged for grant ZWAP 04/007 and for a fellowship to E.B. P.M. thanks Dr. D. Beljonne for useful support and discussions.

JA901636V